Metallophysics and Advanced Technologies
Металофіз. новітні технол.
Metallofiz. Noveishie Tekhnol.
2021, vol. 43, No. 4, pp. 541–551
https://doi.org/10.15407/mfint.43.04.0541
Reprints available directly from the publisher

© 2021 G. V. Kurdyumov Institute for Metal Physics,
National Academy of Sciences of Ukraine
Published by license under
the G. V. Kurdyumov Institute for Metal Physics–
N.A.S. of Ukraine Publishers imprint.
Printed in Ukraine.

ELECTRONIC STRUCTURE AND PROPERTIES

PACS numbers: 62.20.-x, 71.15.Mb, 71.20.Be, 71.20.Nr, 71.27.+a, 72.25.-b, 75.10.Lp

Electronic Structure, Magnetic and Mechanical Properties of MnCoSi Half-Heusler Alloy

S. V. Syrotyuk

Lviv Polytechnic National University,
12 Bandera Str.,
UA-79013 Lviv, Ukraine

In this work the electronic properties of the MnCoSi half-Heusler alloy are evaluated within the formalism of the electron density functional. The calculations are made using ABINIT code in two approaches. They are based on the projector augmented waves (PAW) and on the norm-conserving pseudopotentials (NCPP). The hybrid exchange-correlation functional PBE0, which allows to remove partly the self-interaction of strongly correlated 3*d* electrons of Co and Mn atoms, is implemented on the PAW basis. The electronic energy spectra of the MnCoSi crystal in the magnetic and nonmagnetic phases have been evaluated in the PAW basis states. In the process of optimizing the crystal structure, the interpolants of total energy $E(V)$ and pressure $P(V)$ as the functions of volume, and $V(P)$ as a function of pressure are found. Based on these dependencies, the bulk modulus B_0 = 196.1 GPa is found. As established, in the magnetic state the MnCoSi material is a metal for spin up and a semiconductor for spin down. In the non-magnetic state, the material is a metal. Electronic properties are obtained for the uncompressed and compressed states of the crystal. The pressure dependencies of the magnetic moment of atoms are also found. Within the second approach (NCPP), the elastic constants c_{11}, c_{12}, and c_{44} are calculated, from which the moduli of elasticity, a sound waves velocities, and Debye temperature are derived. The bulk modulus B_0 = 197.1 GPa found in this approach is well compared with one obtained on the PAW basis.

Key words: half-Heusler alloy, structure optimization, electronic structure, ferromagnetic ordering, elastic constants, bulk modulus of elasticity, Debye temperature.

Corresponding author: Stepan Vasylyovych Syrotyuk
E-mail: svsnpe@gmail.com

Citation: S. V. Syrotyuk, Electronic Structure, Magnetic and Mechanical Properties of MnCoSi Half-Heusler Alloy, *Metallofiz. Noveishie Tekhnol.*, **43**, No. 4: 541–551 (2021), DOI: 10.15407/mfint.43.04.0541.

У роботі в рамках формалізму функціонала електронної густини виконано розрахунки електронних властивостей напівгейслерового стопу MnCoSi. Обчислення зроблені за допомогою програми ABINIT в рамках двох підходів. Перший з них ґрунтується на проекційно-приєднаних хвилях (PAW), а другий базується на зберігальних норму псевдопотенціалах. У базисі PAW імплементований гібридний обмінно-кореляційний функціонал PBE0, який дозволяє частково вилучати самодію сильно скорельованих 3d-електронів Co й Mn. У базисі PAW розраховано електронні енергетичні спектри кристала MnCoSi у магнетній і немагнетній фазах. У процесі оптимізування структури кристала знайдено інтерполянти повної енергії $E(V)$ та тиску $P(V)$ як функції об'єму, а також $V(P)$ як функції тиску. На основі цих залежностей знайдено об'ємний модуль пружності $B_0 = 196{,}1$ ГПа. Встановлено, що у магнетному стані матеріял MnCoSi є металом для спіну вгору і напівпровідником для спіну вниз. У немагнетному стані матеріял є металом. Електронні властивості одержано для нестиснутого і стиснутого станів кристала. Знайдені також залежності магнетних моментів атомів як функції тиску. В рамках другого підходу (NCPP) розраховано пружні константи c_{11}, c_{12} та c_{44}, на основі яких були отримані модулі пружності, швидкості звукових хвиль і температура Дебая. Знайдений у цьому підході об'ємний модуль пружності $B_0 = 197{,}1$ ГПа добре узгоджується з отриманим на основі базису PAW.

Ключові слова: напівгейслеровий стоп, оптимізація структури, електронна структура, феромагнетне впорядкування, пружні константи, об'ємний модуль пружності, температура Дебая.

(Received September 24, 2020)

1. INTRODUCTION

Half-Heusler alloys are currently the subject of active multidisciplinary research due to their potential for practical application in the spin electronics [1], thermoelectricity [2] and thermomagnetic energy generation [3]. The structural, electronic and magnetic properties of half-Heusler alloys are studied [1], but there is a very little information about the mechanical properties of these materials in modern literature sources. This is especially true in the case of materials containing transition elements. The spin-polarized calculations of electronic and magnetic properties of half-Heusler alloys make it possible to reveal the half-metallic properties that are important for the potential application of the latter in spin electronics [4].

An example of such a material is MnCoSi, the electronic structure of which is found using ultra-soft pseudopotentials [5], with the cut-off energy of the plane wave basis set of 400 eV.

In a work [5] the subsystem of strongly correlated 3d electrons of Mn and Co atoms is treated with the exchange-correlation potential in the GGA approximation. This approach does not provide a good descrip-

tion of strongly correlated $d(f)$ electrons, which is carried out mainly by the LDA + U method [6] or by means of the hybrid functionals of the exchange-correlation energy, namely the PBE0 [7] or HSE06 [8]. Recently we have found that the use of the hybrid functional PBE0 leads to a better comparison with the experiment of kinetic coefficients in sphalerite ZnSe material [9]. The hybrid HSE06 functional, combined with the Green's function approach, led to excellent agreement with the measured band gaps for the wurtzite crystals ZnX (X = O, S, Se, Te) [10]. It is established that the use of the hybrid functional PBE0 provides better comparison of the band gap in the solid solution CdMnTe [11] with the experiment [12]. In addition, the elastic properties of the MnCoSi crystal have not yet been studied. The study of the dependence of the magnetic moment of an elementary cell on pressure is also one of the tasks of this work. The electronic structure of the MnCoSi crystal is calculated in the free and compressed states. Let's turn to the solution of these tasks.

2. THEORETICAL DETAILS

The electronic structure of MnCoSi material is calculated on the basis of projector augmented waves (PAW) [13] by means of the ABINIT code [14]. The hybrid exchange-correlation functional PBE0 [15], suitable for a realistic description of strongly correlated 3d electrons of the Mn and Co, is included into calculation scheme. The hybrid functional PBE0 is given by the formula

$$E_{xc}^{\mathrm{PBE0}}[\rho] = E_{xc}^{\mathrm{PBE}}[\rho] + \alpha(E_x^{\mathrm{HF}}[\Psi_{3d}] - E_x^{\mathrm{PBE}}[\rho_{3d}]), \quad (1)$$

in which the first term is the energy in the GGA–PBE approximation [16]. The electronic properties of the MnCoSi crystal are calculated on the basis of the GGA–PBE and PBE0 functionals. In the first approach, the mixing coefficient $\alpha = 0$ in Eq. (1). The corresponding results are shown in Figs. 1 and 4. If the parameter $\alpha \neq 0$, then the corresponding exchange-correlation functional (1) includes the exact Hartree–Fock exchange energy, in which the self-interaction error is partly removed. The PBE0 functional shows the better description of the electronic structure in materials, containing $d(f)$ electrons.

We consider here the crystal, which is described by the space group $F43m$ (216). The reduced coordinates of the atoms in a primitive cell are as follows: Mn (0, 0, 0), Co (0.25, 0.25, 0.25), and Si (0.5, 0.5, 0.5). The electronic structure is calculated on plane waves with a maximum kinetic energy of 1088 eV, but energy of 1632 eV is used for mechanical properties. The integration is performed on a Monkhorst–Pack grid 8×8×8, which provided 29 points in the irreducible part of the Brillouin zone. The initial value of the crystal lattice parameter in the nonmag-

netic state had a value of 5.36 Å, and the optimized parameter is calculated to be 5.329 Å. The corresponding pressures in the crystal are –3.2626 GPa and $1.0629 \cdot 10^{-9}$ GPa, respectively. The elastic properties of the crystal are calculated in the spin-polarized state on the NCPP [17].

The mechanical properties of a cubic crystal are determined by three independent elastic constants [18] namely, c_{11}, c_{12}, and c_{44}. And from them the bulk modulus is calculated, $B = (c_{11} + 2c_{12}) / 3$. The modules of Voight, $G_V = (c_{11} - c_{12} + 3c_{44})/5$, Reuss, $G_R = \dfrac{5(c_{11} - c_{12})c_{44}}{4c_{44} + 3(c_{11} - c_{12})}$, and Hill, $G_H = (G_V + G_R)/2$ are also defined by these three constants. The shear (transverse), $\upsilon_s = \sqrt{G/\rho}$, and compressional sound velocity $\upsilon_p = \sqrt{(3B + 4G)/(3\rho)}$ define the average value, $\upsilon_m = [(2\upsilon_s^{-3} + \upsilon_p^{-3})/3]^{-1/3}$. The last parameter allows to find the Debye temperature, $T_D = \upsilon_m \dfrac{h}{k}\left[\dfrac{3}{4\pi V}\right]^{1/3}$, where h and k denotes the Plank's and Boltzmann's constant, respectively, and V is the unit cell volume.

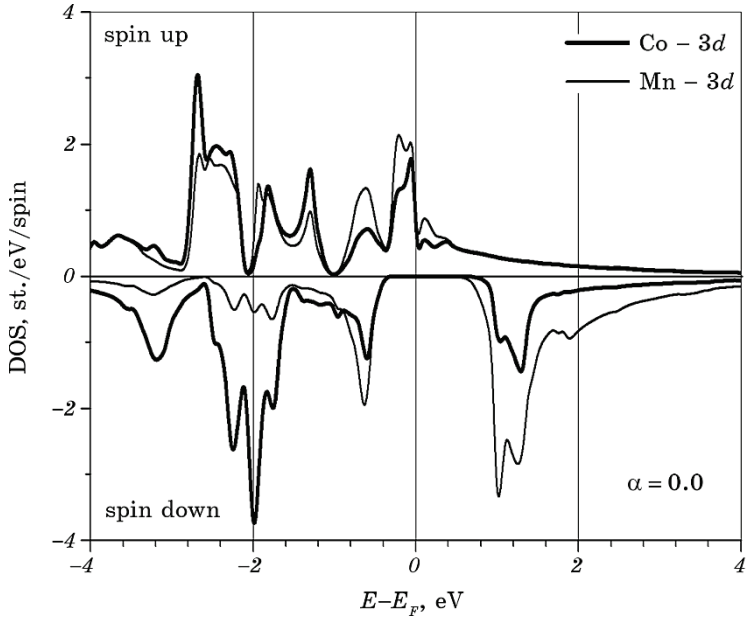

Fig. 1. Partial density of the 3*d* electronic states of Co and Mn atoms in MnCoSi material, found with the cell volume of V_0 = 153.99 Å^3, using the GGA–PBE exchange-correlation functional.

3. RESULTS AND DISCUSSION

The structural, electronic and magnetic properties of the MnCoSi crystal found here for ferromagnetic state are collected in a Table 1. The electronic properties of the MnCoSi crystal are calculated on the basis of PAW functions based on the GGA–PBE and PBE0 exchange-correlation energy functionals. The results corresponding to the GGA–PBE approach ($\alpha = 0$) are shown in Figs. 1 and 4. The results corresponding to the values of the parameter $\alpha \neq 0$ are shown in Figs. 2, 3, 5, and 6. Figs. 1–3 represent the partial densities 3*d* of electrons Co and Mn found in a crystal with a normal unit cell volume.

Figures 4–6 show the results for the compressed crystal under the action of external hydrostatic pressure. Figure 1 shows the spin-polarized partial densities of the Co and Mn 3*d* electrons, obtained without taking into account the strong correlations of 3*d* electrons. We see that for the spin down the material is a semiconductor, and the Fermi level is located closer to the top of the valence band. For the spin up, the material exhibits metallic properties. And now we partially remove the self-interaction of 3*d* electrons from the exchange-correlation functional, including in the consideration the Hartree–Fock exchange in Eq. (1) with the coefficient $\alpha = 0.0625$. A comparison of Figures 1 and 2 shows that taking into account the strong correlations with a small impurity of Hartree–Fock energy led to a noticeable redistribution of the density of electronic states. The Fermi level has now become closer to the top of the valence band. Figures 1 and 2 show that for spins up we have a metallic state, and near the Fermi level 3*d* states of the Co and Mn are dominating.

Figure 3 represents the density of electronic 3*d* states of Co and Mn, calculated for the material at normal pressure ($P = 0$). It is seen that the Fermi level crosses the state density curves for both spin orientations. So, there is now a pseudo-gap in the energy spectrum for electrons with the spin down.

How will the density of electronic states in the material change under the action of external hydrostatic pressure? The answers to this question will be obtained by analyzing the results shown in Figs. 4–6.

TABLE 1. The electronic and magnetic properties of the half-Heusler MnCoSi compound, found for a ferromagnetic phase (FM). Parameter $\delta E = E_{FM} - E_{NM}$ is a difference of the total energy in FM and non-magnetic (NM) phase.

Phase	α	a, Å	δE, eV	m^{tot}, μ_B	m^{Co}, μ_B	m^{Mn}, μ_B	m^{Si}, μ_B	E_g, eV
FM	0.0	5.39	–0.42	2.000	–0.008	2.137	–0.040	0.76
FM	0.125	5.53		2.813	–0.577	3.384	–0.032	1.20
FM [4]		5.41	–0.44	2.00	–0.04	2.12		0.64

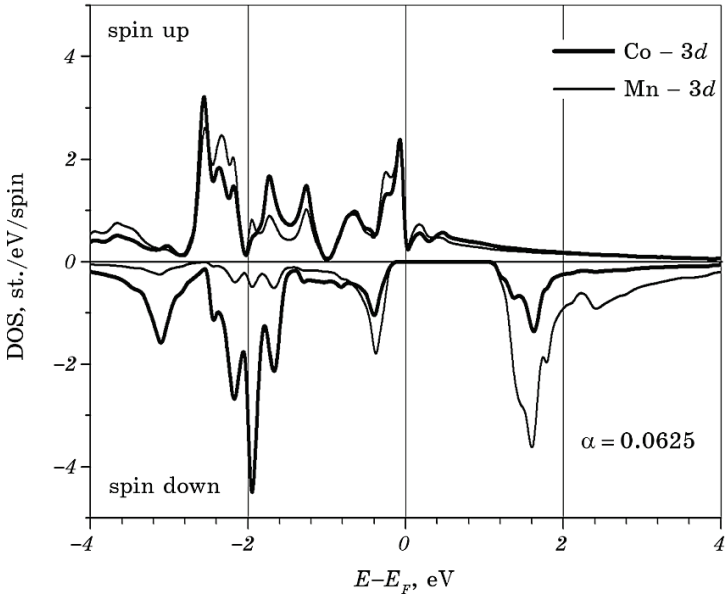

Fig. 2. Partial density of the 3*d* electronic states of Co and Mn atoms in MnCoSi material, found with the cell volume of $V_0 = 153.99$ Å^3, using the hybrid PBE0 exchange-correlation functional.

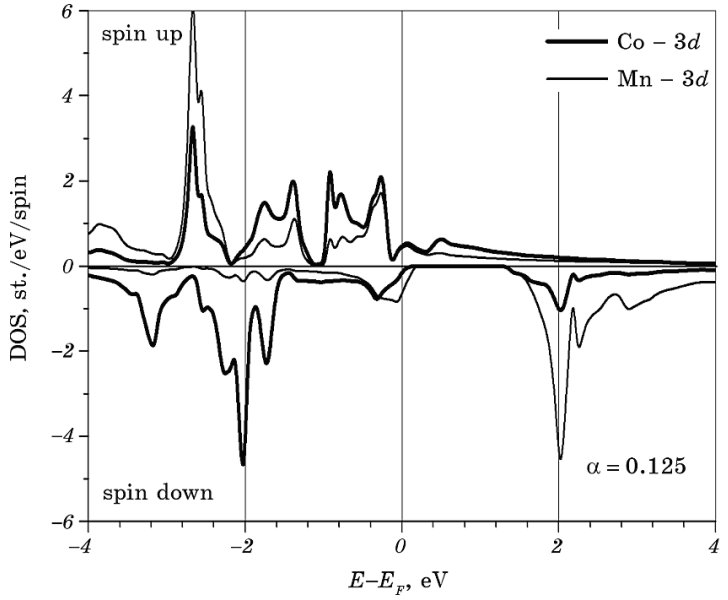

Fig. 3. Partial density of the 3*d* electronic states of Co and Mn atoms in MnCoSi material, found with the cell volume of $V_0 = 153.99$ Å^3, using the hybrid PBE0 exchange-correlation functional.

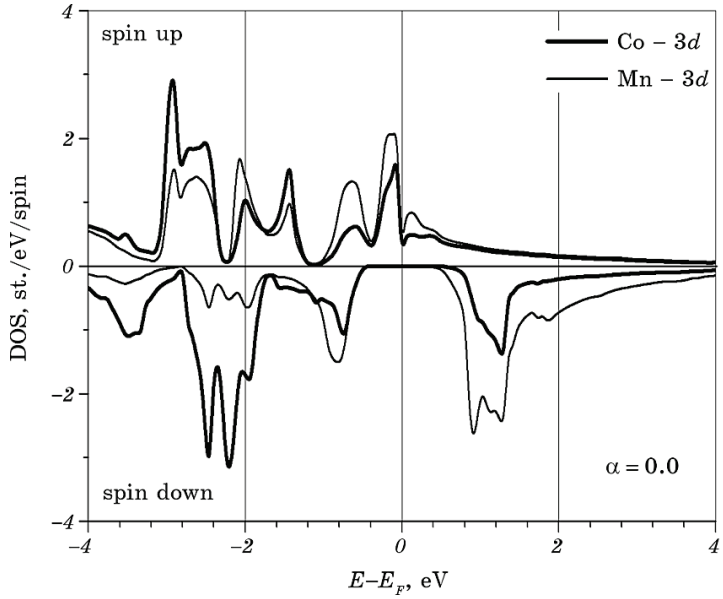

Fig. 4. Partial density of the 3*d* electronic states of Co and Mn atoms in MnCoSi material, found with the cell volume of V = 144.93 Å^3, using the GGA–PBE exchange-correlation functional.

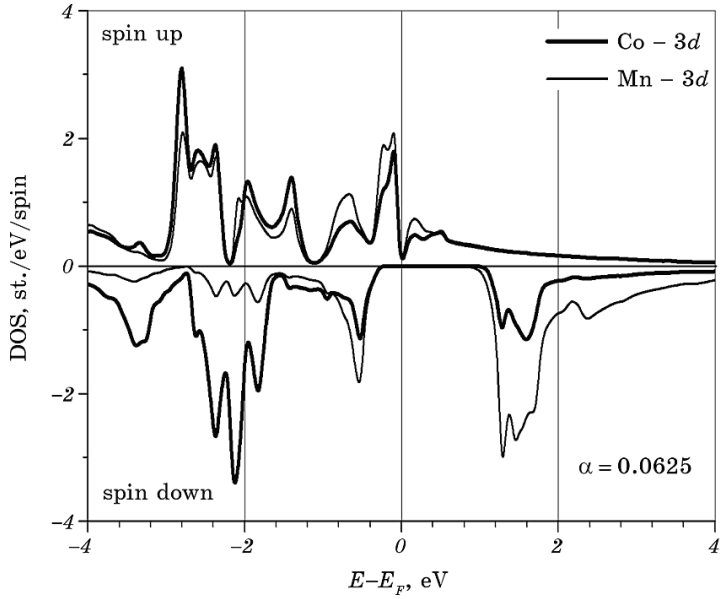

Fig. 5. Partial density of the 3*d* electronic states of Co and Mn atoms in MnCoSi material, found with the cell volume of V = 144.93 Å^3, using the hybrid PBE0 exchange-correlation functional.

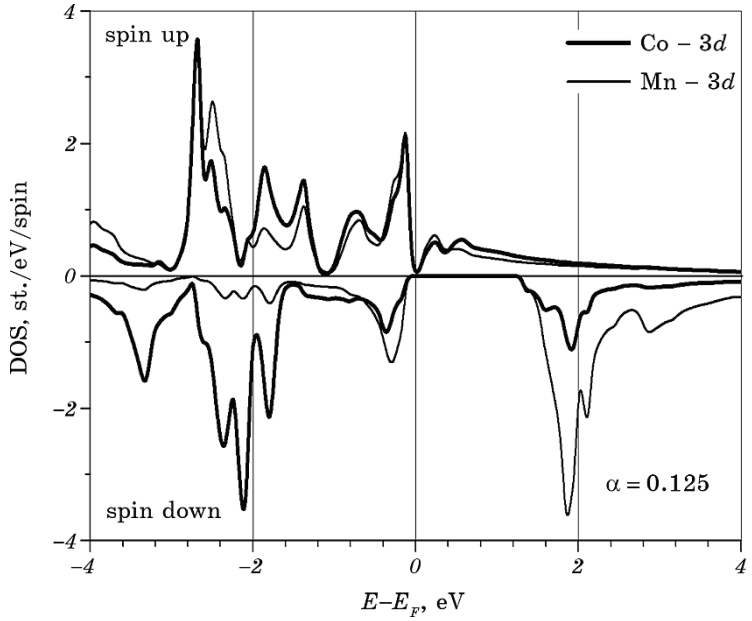

Fig. 6. Partial density of the 3*d* electronic states of Co and Mn atoms in MnCoSi material, found with the cell volume of $V = 144.93$ Å^3, using the hybrid PBE0 exchange-correlation functional.

Comparing Fig. 1 (the free crystal) and 4 (the compressed crystal), we conclude that the compressed crystal exhibits half-metallic properties. The Fermi level of the compressed crystal is in the middle of the band gap for spin down.

The partial densities of the electronic states shown in Figs. 2 and 5 reveal the semi-metallic state in the material. The Fermi level is localized close to the top of the valence band.

Figures 3 and 6 show for the spin down states the pseudo-gap in the free crystal and the semiconductor band gap in the compressed, respectively.

Now consider the behaviour of the magnetic moments of atoms in a MnCoSi crystal found with the GGA–PBE potential when the value of the mixing parameter is $\alpha = 0$. Note that the external hydrostatic pressure has almost no effect on the value of the total magnetic moment of the unit cell, $M = 2\ \mu_B$. Figure 7 shows that the magnetic moment of the Mn atom decreases, and at the Co atom, on the contrary, increases. The magnetic moment of the Si atom is negative and almost constant.

For the strongly correlated electron subsystem, the PBE0 functional is more adequate. The corresponding results are shown in Fig. 8, the corresponding data of which are calculated with a mixing coefficient $\alpha = 0.125$. This Figure shows that the total magnetic moment of the

unit cell decreases with the pressure increasing. From Figure 7 we see that the largest magnetic moments of Mn and Co atoms are parallel without taking into account strong correlations of $3d$ electrons ($\alpha = 0$), and taking into account the latter ($\alpha = 0.125$) leads to their antiparallel moments for the crystal in the compressed state (Fig. 8).

The mechanical stability in cubic crystals on the elastic constants are given by conditions $c_{11} - c_{12} > 0$, $c_{11} > 0$, $c_{44} > 0$, $c_{11} + 2c_{12} > 0$, and $c_{44} < B < c_{11}$. As can be seen from Table 2 all these conditions are satisfied confirming the stability of the crystal structure under consideration. The Pough criteria [19] $B/G > 1.75$, and the Frantsevich criteria [19]

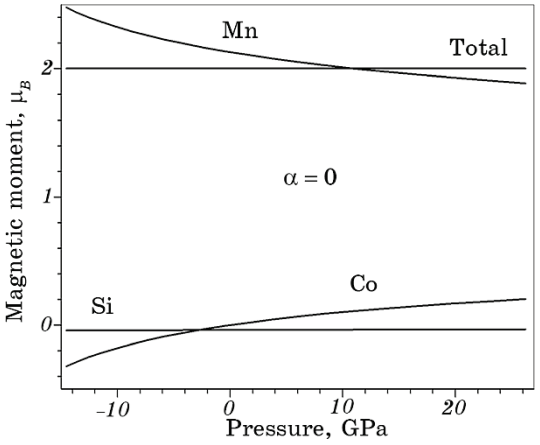

Fig. 7. Magnetic moments at atoms versus pressure obtained without the Hartree–Fock admixture in the exchange-correlation functional PBE0.

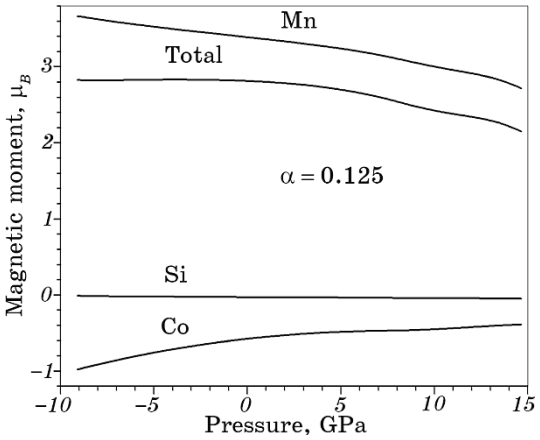

Fig. 8. Magnetic moments at atoms versus pressure obtained with the Hartree–Fock admixture in the exchange-correlation functional PBE0.

TABLE 2. The elastic properties of the half-Heusler MnCoSi compound. The sound velocities are evaluated with the Hill module G_H.

c_{11}, GPa	c_{12}, GPa	c_{44}, GPa	B, GPa	B', GPa	B'', GPa	G_V, GPa	G_R, GPa	G_H, GPa	v_p, m/s	v_s, m/s	v_m, m/s	θ, K	B/G
276.7	157.7	127.5	197.1	4.508	–0.026	100.2	87.3	93.8	7254	3913	4368	385	2.1

$G/B < 0.57$, so the material shows ductility.

We also found third- and fourth-order pressure derivatives of the bulk modulus, namely $B^{(3)} = -0.0012$, $B^{(IV)} = -0.000036$ GPa, respectively. So, we have the corresponding Taylor series, namely $B(P) = B + B'P + (1/2)B''P^2 + (1/6)B^{(3)}P^3 + (1/24)B^{(IV)}P^4$, where the B, B', and B'' are given in a Table 2.

4. CONCLUSION

1. The electronic structure of the MnCoSi half-Heusler alloy is calculated. The results for free and compressed crystals are obtained using exchange-correlation energy in the approximations of GGA and hybrid PBE0 functional, respectively. It is found that the MnCoSi material in the ferromagnetic state has a lower total energy than in the nonmagnetic one. It is found that in the ferromagnetic state the material is a half-metal, while its nonmagnetic phase is metallic.
2. The magnetic moments of the unit cell and atoms are found using the GGA and PBE0 functionals. The dependences of the magnetic moments on the pressure are also calculated. The magnetic moments, found here, show that the material is characterized by a noncollinear spiral magnetic ordering.
3. It is established that the external hydrostatic pressure leads to a significant redistribution of the partial densities of 3d electrons of the Co and Mn atoms. Partial elimination of the self-interaction error ($\alpha \neq 0$) in the subsystem of strongly correlated 3d electrons leads to a significant increase in the band gap for electrons with spins down.
4. The modules of elasticity, velocity of sound waves and Debye temperature are obtained from the elastic constants found here. The bulk modulus, derived from elastic constants, compares well with that obtained from the dependence of the total energy on volume calculated here, $E(V)$. This confirms that the calculated elastic constants are feasible and reliable. The pressure derivatives B', B'', B''', and $B^{(IV)}$ of bulk modulus also are found. The Pough and Frantsevich criteria indicate that MnCoSi is ductile.

ACKNOWLEDGEMENT

This contribution is created under the support of the High Perfor-

mance Computing Laboratory at the Lviv Polytechnic National University.

REFERENCES

1. J. Ma,V. I. Hegde, K. Munira, Y. Xie, S. Keshavarz, D. T. Mildebrath, C. Wolverton, A. W. Ghosh, and W. H. Butler, *Phys. Rev. B*, **95**, Iss. 2: 024411 (2017).
2. S. J. Poon, *Metals*, **8**: 989 (2018).
3. E. E. Levin, J. D. Bocarsly, J. H. Grebenkemper, Ramsey Issa, S. D. Wilson, T. M. Pollock, and R. Seshadri, *APL Mater.*, **8**: 041106 (2020).
4. V. N. Uvarov, N. V. Uvarov, and M. V. Nemoshkalenko, *Metallofiz. Noveishie Tekhnol.*, **41**, No. 11: 1409 (2019) (in Russian).
5. L. Feng, E. K. Liu, W. X. Zhang, W. H. Wang, and G. H. Wu, *J. Magn. Magn. Mater.*, **351**: 92 (2014).
6. V. N. Antonov and V. P. Antropov, *Low Temp. Phys.*, **46**: 1 (2020).
7. J. P. Perdew, M. Ernzerhof, and K. Burke, *J. Chem. Phys.*, **105**: 9982 (1996).
8. J. Heyd, G. E. Scuseria, and M. Ernzerhof, *J. Chem. Phys.*, **118**: 8207 (2003).
9. O. P. Malyk and S. V. Syrotyuk, *J. Electron. Mater.*, **47**: 4212 (2018).
10. S. V. Syrotyuk and O. P. Malyk, *J. Nano- Electron. Phys.*, **11**, No. 6: 06018 (2019).
11. S. V. Syrotyuk and O. P. Malyk, *J. Nano- Electron. Phys.*, **11**, No. 1: 01009 (2019).
12. R. Yu. Petrus, H. A. Ilchuk, V. M. Sklyarchuk, A. I. Kashuba, I. V. Semkiv, and E. O. Zmiiovska, *J. Nano- Electron. Phys.*, **10**, No. 6: 06042 (2018).
13. P. E. Blőchl, *Phys. Rev. B*, **50**: 17953 (1994).
14. X. Gonze, F. Jollet, F. Abreu Araujo, D. Adams, B. Amadon, T. Applencourt, C. Audouze, J.-M. Beuken, J. Bieder, A. Bokhanchuk, E. Bousquet, F. Bruneval, D. Caliste, M. Côté, F. Dahm, F. Da Pieve, M. Delaveau, M. Di Gennaro, B. Dorado, and C. Espejo, *Comput. Phys. Commun.*, **205**: 106 (2016).
15. E. Tran, P. Blaha, K. Schwarz, and P. Novák, *Phys. Rev. B*, **74**: 155108 (2006).
16. J. P. Perdew, K. Burke, and M. Ernzerhof, *Phys. Rev. Lett.*, **77**: 3865 (1996).
17. M. J. van Setten, M. Giantomassi, E. Bousquet, M. J. Verstraete, D. R. Hamann, X. Gonze, and G.-M. Rignanese, *Comput. Phys. Commun.*, **226**: 39 (2018).
18. X. Gonze and C. Lee, *Phys. Rev. B*, **55**: 10355 (1997).
19. M. K. Hussain, *Spin*, **9**: 1950018 (2019).